Turkish Journal of Earth Sciences (Turkish J. Earth Sci.), **Vol. 11**, 2002, pp. 193-203. *Copyright ©TÜBİTAK*

The Role of Crustal Fluids in Strike-slip Tectonics: New Insights from Magnetotelluric Studies

MARTYN UNSWORTH

Institute of Geophysical Research, University of Alberta, Edmonton, Alberta, T6G 2J1, Canada
(e-mail: Unsworth@phys.UAlberta.ca)

Abstract: The presence of fluids in the Earth's crust can dramatically change the rheology and may control a wide range of tectonic processes, especially in regions characterized by strike-slip deformation. Fluids such as water and partial melt change the electrical resistivity of the subsurface and may be detected through geophysical techniques that remotely sense electrical resistivity. For imaging to crustal and upper mantle depths, the most useful technique is magnetotellurics (MT) that uses natural electromagnetic waves as an energy source. Magnetotelluric studies of the Tibetan Plateau have detected a widespread mid-crustal layer of partial melting across almost the entire north-south extent of the plateau. This provides a locus for deformation that decouples the upper and lower parts of the lithosphere and allows the continued convergence of India and Asia to extrude the Asian lithosphere to the east. The melt layer terminates at the North Kunlun fault, one of the major strike-slip faults that accommodate the eastward extrusion. A detailed magnetotelluric study of the San Andreas Fault in Central California has imaged a wedge of fractured, fluid-saturated rock in the upper 3–5 km of the fault zone. The micro-earthquake distribution shows that seismicity begins at the base of this zone. Fault segments with a higher fluid budget exhibit creep, while the relatively dry fault segments are generally locked.

Key Words: crustal fluids, magnetotelluric, strike-slip tectonics, transform plate boundaries, crustal deformation

Yerkabuğu'ndaki Akışkanların Doğrultu-atımlı Tektonizma Üzerindeki Rolü: Manyetotellürik Çalışmaların Işığında Yeni Bulgular

Özet: Akışkanların yerkabuğu içindeki varlıkları reolojik özellikleri (fiziksel ve kimyasal özellikleri) değiştirip, bir dizi tektonik olayları kontrol edebilirler. Su ve kısmi ergimeye uğramış eriyikler gibi akışkanlar yeryüzüne yakın kesimlerdeki elektrik özdirenç değerlerini değiştirir ve bu değişimler jeofizik teknikler, uzaktan gözlenebilecek elektrik özdirenç değerlerinin izlenmesi gibi, ile algılanabilirler. Kabuk ve üst manto'ya kadar inebilecek derinlikleri incelemek için en kullanışlı tekniklerden biri de doğal elektromanyetik alanı kaynak olarak kullanan manyetotellürik yöntemdir. Tibet platosunu Kuzey–Güney doğrultusunda boydan boya kesen profiller boyunca yapılan manyetotellürik gözlemlerinde, kabuğun orta kesimlerinde yer alan kısmi ergimeye uğramış geniş alanlara dagılmış bir tabaka gözlenmiştir. Bu gözlem, litosferin üst ve alt kesiminde deformasyonun kaynaştığı (iç-içe geçmesi) bir bölgenin oluşumunu ve Hindistan ile Asya levhalarının süregelen etkileşiminde Asya litosferinin doğu'ya kaçışına olanak sağlar. Akışkan (ergiyik) tabaka, doğuya yönelen tektonik hareketleri kontrol eden en önemli doğrultu-atımlı faylardan biri olan Kuzey Kunlun Fayı'nda son bulur. San Andreas Fayı'nda (Orta Kaliforniya) yapılan detaylı manyetotellürik araştırmalar sonucunda fay zonunun yaklaşık olarak ~3–5 km derinliğindeki üst kesiminde akışkanlarca oldukça doygun, kırıklı kama şeklinde bir yapı gözlenmiştir. Mikrodepremlerin dağılımları sismisitenin bu zonun altından itibaren başladığını göstermektedir. Kuru Fay (kırık) parçacıkları genelde tektonik yükler altında kilitlenirken, yüksek oranda suya (akışkan) doygun fay parçacıkları akma, yamulma şeklindeki deformasyonlara uğrarlar.

Anahtar Sözcükler: yerkabuğundaki akışkanlar manyetotellürik, doğrultu-atımlı tektonizma, transform kıta kenarı, yerkabuğu deformasyonu

Introduction

Understanding the physical processes that control continental dynamics requires information about the physical state of the Earth's crust and mantle in regions where tectonic processes are at work. Geophysical imaging plays a crucial role in this respect. Seismic exploration is the most widely used technique and yields estimates of seismic velocities that are interpreted in terms of the composition of the crust and mantle. Additional information can be obtained from sub-surface electrical resistivity that is imaged with electromagnetic geophysical techniques. Since electrical resistivity is sensitive to the presence of fluids, it provides a valuable complement to seismic studies. In this paper the basis of the magnetotelluric (MT) method is reviewed, and then results from two magnetotelluric studies of regions undergoing strike-slip tectonics are presented. In the first magnetotellurics is used to image lithospheric structure in Tibet, where major strike-slip faults have developed in response to the continued convergence between India and Asia. In the second study MT has been used to obtain detailed images of the internal structure of the San Andreas Fault in California.

The Magnetotelluric Method

The electrical resistivity of the Earth's interior contains information about its composition and structure. Naturally occurring rocks and minerals exhibit a very wide range of electrical resistivities. Crystalline igneous rocks typically have resistivities greater than 1000 ohm-m, sedimentary rocks have intermediate resistivities and fluid saturated rocks and ore bodies can exhibit resistivities below 1 ohm-m. These resistivity values are strongly influenced by the presence of interconnected aqueous or magmatic fluids in the pores of the rock. Thus remotely sensing the electrical resistivity of the subsurface can constrain its physical state and fluid content. Note that in this paper both electrical resistivity and electrical conductivity are used to describe the properties of the Earth's interior. A wide range of electromagnetic (EM) geophysical techniques can be used to map subsurface resistivities. Many of these techniques require electromagnetic waves to be generated by a transmitter. The magnetotelluric method utilizes naturally occurring electromagnetic waves to probe the earth, thus avoiding the technical problems and cost of generating artificial signals. Man-made signals are generally too weak to image below a depth of 10 km, and exploration below this depth can only be achieved with natural EM signals. The magnetotelluric method maps the variation of electrical resistivity with depth by means of the skin depth effect. The amplitude of an electromagnetic wave will decay with a characteristic skin depth

$$d = 503\sqrt{\frac{\rho}{f}}$$

where ρ is the resistivity of the ground (ohm-m), f is the frequency (Hz) and d the skin depth (m). This attenuation occurs as the electromagnetic energy is dissipated in the earth as heat through ohmic losses. This equation shows that low frequency electromagnetic waves have a larger skin depth and thus penetrate deeper into the Earth than high frequency electromagnetic waves (Figure 1). High frequency EM waves (frequencies above 1 Hz) typically originate in world wide lightening activity and their small skin depth gives information about resistivity structure close to the surface. As the frequency decreases, the electromagnetic wave penetrates deeper into the earth and senses resistivity at greater depths. These lower frequency (1–0.00001 Hz) electromagnetic waves originate in magnetospheric oscillations caused by the solar wind. It can be shown that the apparent resistivity, ρ_a, of the earth is given by

$$\rho_a = \frac{1}{2\pi f \mu_0}\left|\frac{E}{H}\right|^2$$

where E and H are mutually orthogonal, horizontal, electric and magnetic fields at the earths surface and μ_0 is the magnetic permeability of free space. If the earth has a uniform electrical resistivity, the apparent resistivity is equal to the true electrical resistivity. However, if the subsurface resistivity structure is not homogeneous, the apparent resistivity represents an average resistivity from the surface to a depth of a skin depth. Figure 2 shows a two-layer electrical resistivity model and the variation of apparent resistivity with frequency that would be measured on the Earth's surface by an MT instrument. At frequencies above 10 Hz, the apparent resistivity is equal to 10 ohm-m, since the electromagnetic energy does not reach the lower layer. As the frequency is reduced, electromagnetic energy penetrates the more resistive lower layer and the apparent resistivity rises. At very low frequency the apparent resistivity asymptotically approaches 100 ohm-m, the true resistivity of the lower

half space. Further details of the basic theory of magnetotellurics for a 1-D Earth are described by Cagniard (1953).

Magnetotelluric data is collected by recording natural variations of the Earth's electric and magnetic fields, and then using a Fourier transform to determine the electric and magnetic fields as a function of frequency. By recording MT for one day it is usually possible to measure EM signals in the frequency range 1000-0.001 Hz. To record lower frequencies (for deep exploration) data must be collected for 1–4 weeks at each measurement location. Once MT data has been collected at a number of stations on a profile or grid of points, it is inverted to generate a model of subsurface resistivity. This converts the apparent resistivity and phase as a function of frequency into true electrical resistivity as a function of depth. This is exactly analogous to the techniques used to convert seismic data from travel times to true depth. Two-dimensional (2-D) modeling and inversion of MT data is now considered standard and three-dimensional modeling and inversion has become tractable in recent years. Additional details of the field techniques and data analysis for the magnetotelluric method are described by Vozoff (1991) and Unsworth (1999).

Magnetotelluric Studies of the India-Asia Collision Zone

The Tibetan plateau is the largest region of thickened and elevated crust on Earth and a direct consequence of the ongoing India-Asia collision (Molnar *et al.* 1993). Knowledge of the structure and evolution of the plateau has advanced through the systematic geological and geophysical studies that began in the 1980s with the Sino-French collaboration in southern Tibet. Magnetotelluric (MT) data were collected during this project and detected unusually high electrical conductivity in the crust (van Ngoc *et al.* 1986). In combination with the high heat flow reported by Francheteau *et al.* (1984), the high conductivity was attributed to the presence of partial melt in the Tibetan crust. In 1995 Project INDEPTH (International Deep Profiling of Tibet and the Himalaya) acquired additional MT data that confirmed the presence of a widespread zone of high conductivity in the middle crust in southern Tibet (Chen *et al.* 1996; 100-line in Figure 3). The top of the conductor was at a depth of 15–20 km, and coincident with seismic bright spots and a seismic low velocity zone (Brown *et al.* 1996; Kind *et al.* 1996; Makovsky & Klemperer 1999). These observations gave further support to the idea that the high conductivity layer represents partial melt in the

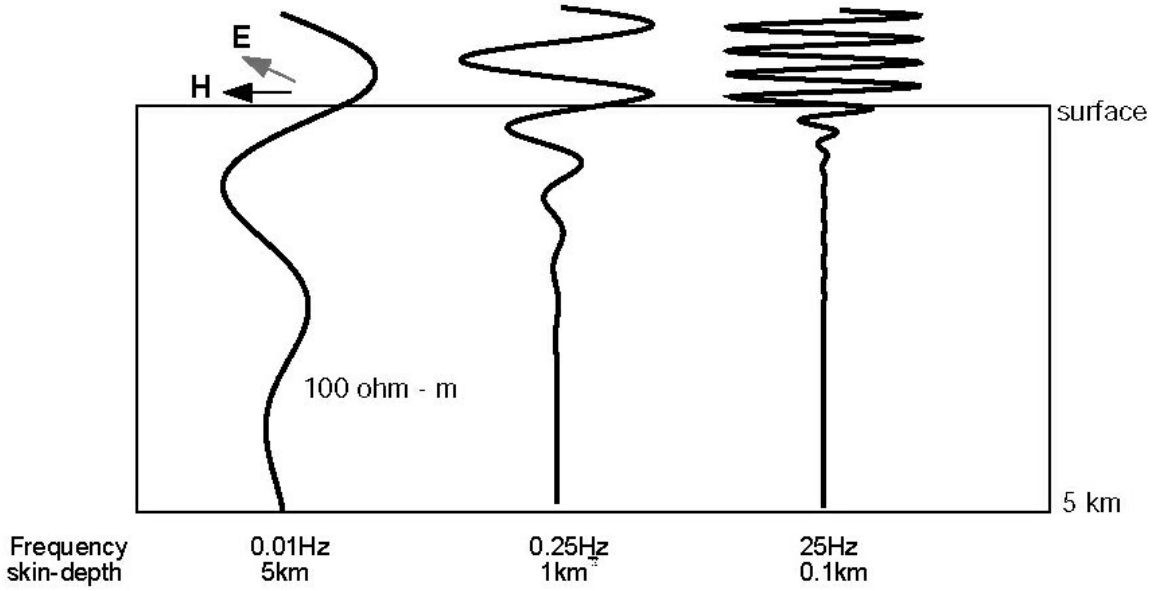

Figure 1. Physics of the magnetotelluric method. Electromagnetic waves penetrate a distance into the Earth that is inversely proportional to frequency. At each frequency the ratio E/H determines the average electrical resistivity over a skin depth. By combining measurements at many frequencies, the depth variation of resistivity is obtained.

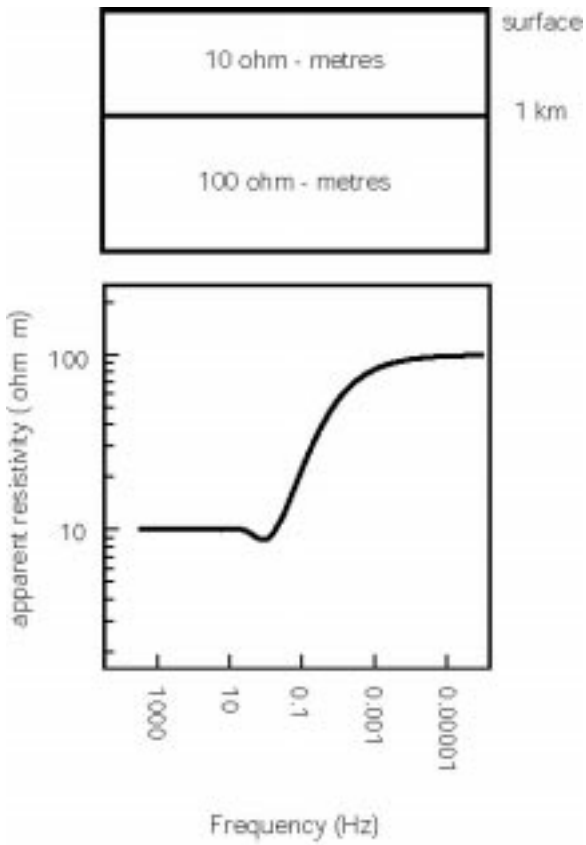

Figure 2. The magnetotelluric response of a simple two-layer resistivity model. Note that as the frequency decreases, the apparent resistivity indicates the presence of the high resistivity basement.

Tibetan crust (Nelson *et al.* 1996). Additional MT data were collected in 1998 and 1999 to examine the spatial extent of this conductive zone (500 and 600 lines, Figure 3). A characteristic feature of the Tibetan MT data is that the apparent resistivities decrease with decreasing frequency, implying that electrical conductivity increases with depth. This response is observed at most MT sites in Tibet, and is markedly different to that observed in stable continental regions worldwide, which typically show increasing apparent resistivities at low frequency.

The INDEPTH MT time series data were processed to obtain estimates of the magnetotelluric impedance tensor using the technique of Egbert (1997) and analyzed with tensor decomposition to determine if a two-dimensional interpretation is valid (McNeice & Jones 2001). The tensor decomposition suggests that at most measurement sites in Tibet, the magnetotelluric data can be reliably interpreted with two-dimensional geoelectric models. The MT data from each profile were then converted into the 2-D conductivity models shown in Figure 4 using the inversion algorithm of Rodi & Mackie (2001). Both the transverse magnetic (TM) mode and vertical magnetic fields were used in these inversions. The main feature observed in the models is that below 20–30 km the crust is highly conductive across the entire Tibetan plateau from the Himalaya to the Kunlun Shan. MT data is most sensitive to the depth and conductance of a conductive layer (conductance is the vertically integrated conductivity). In Tibet the conductance in the mid and lower crust is one to two orders of magnitude higher than in stable continental regions (Jones 1992). The conductance in Tibet locally exceeds 10,000 Siemens in the vicinity of the Yarlung-Tsangpo suture (100-line) and at 33.5°N in the Qiangtang Terrane (600-line).

What is the cause of the unusually high conductivity in the Tibetan crust? Metallic ores, carbon films, partial melt and brines can all produce high crustal conductivities. In each case an essential requirement is that the conducting phase be electrically connected over the area of the observed high conductivity. While metallic ore bodies can produce very high electrical conductivities, they do not have spatial dimensions comparable to those observed in Tibet. The preferred explanation for the high conductance observed beneath Tibet is that widespread fluids are present in the Tibetan crust. The fluid could be distributed partial melt, aqueous fluids, or a combination of both partial melt and aqueous fluids. Interpretation of the electrical conductivity of the crust and mantle has advanced through laboratory studies of the electrical properties of fluid-rock mixtures. These studies have shown that the bulk electrical conductivity of a fluid-bearing rock depends on the electrical conductivity of the fluid, its geometry, and the amount of fluid. Other laboratory studies have shown that basaltic, andesitic, and granitic melts have electrical conductivities ranging from about 4 to 10 S/m (Partsch *et al.* 2000; Olhoeft 1986). The melt phase generally becomes interconnected at low melt fractions (Roberts & Tyburczy 2000) and significantly lowers the overall electrical conductivity of the rock. To quantify the amount of fluid needed to account for the conductances observed in Tibet, consider a rock that contains melt with a conductivity of 10 S/m. If the rock contains 10% of this melt by volume, then the overall rock conductivity would be 0.6 S/m. A layer of this partially molten rock would need to be 16 km thick to

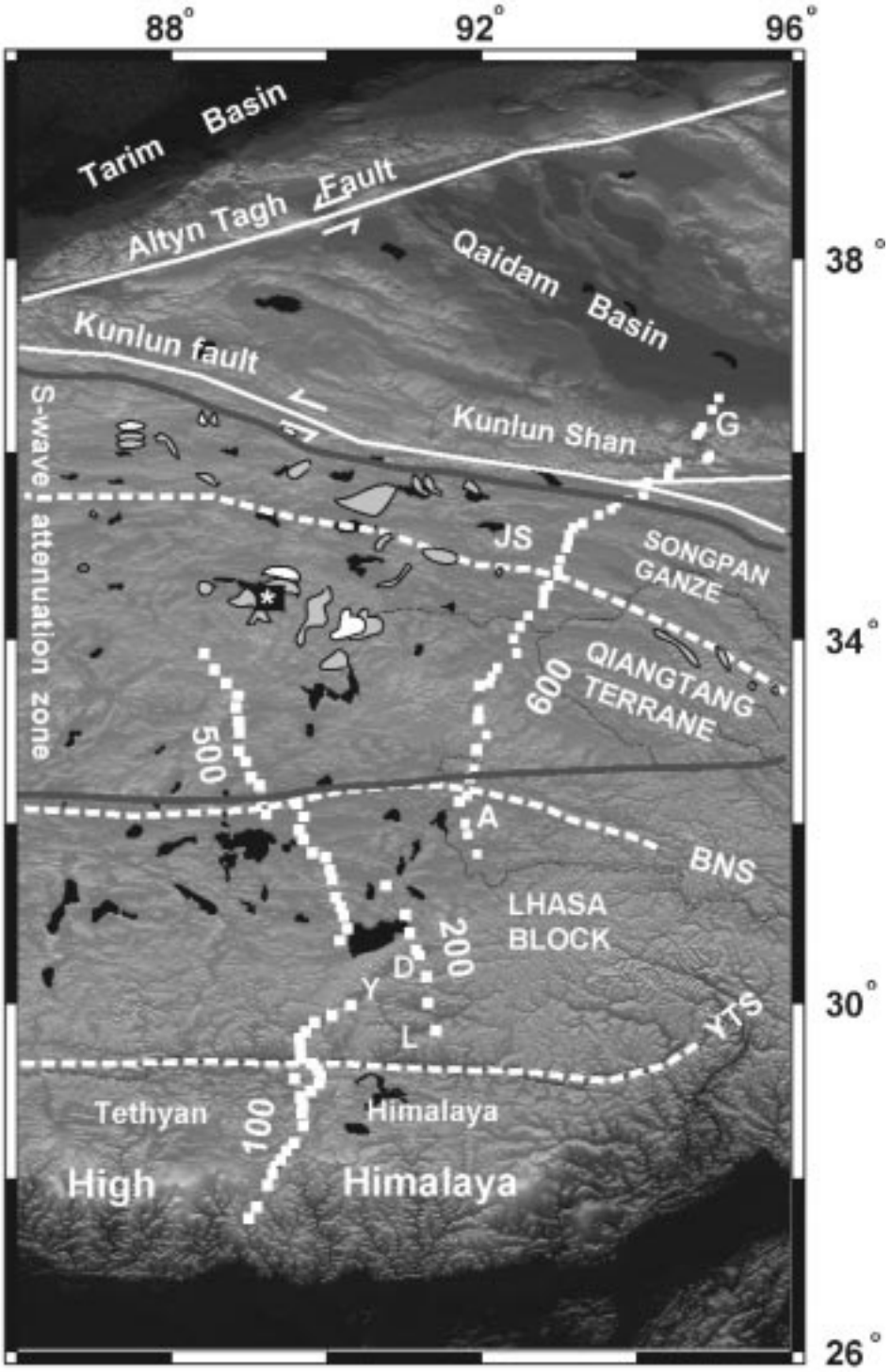

Figure 3. Tectonic setting of the INDEPTH magnetotelluric profiles on the Tibetan Plateau. The numbers indicate the name of each profile. YTS– Yarlung Tsangpo suture, BNS– Bangong-Nuijang suture, JS– Jinsha suture. White denotes volcanic rocks younger than 5 My and light gray denotes older than 5 My or undated. The xenolith location described by Hacker *et al.* (2000) is shown by the asterisk. The zone of seismic shear wave attenuation described by Owens and Zandt (1997) is bounded by the red line.

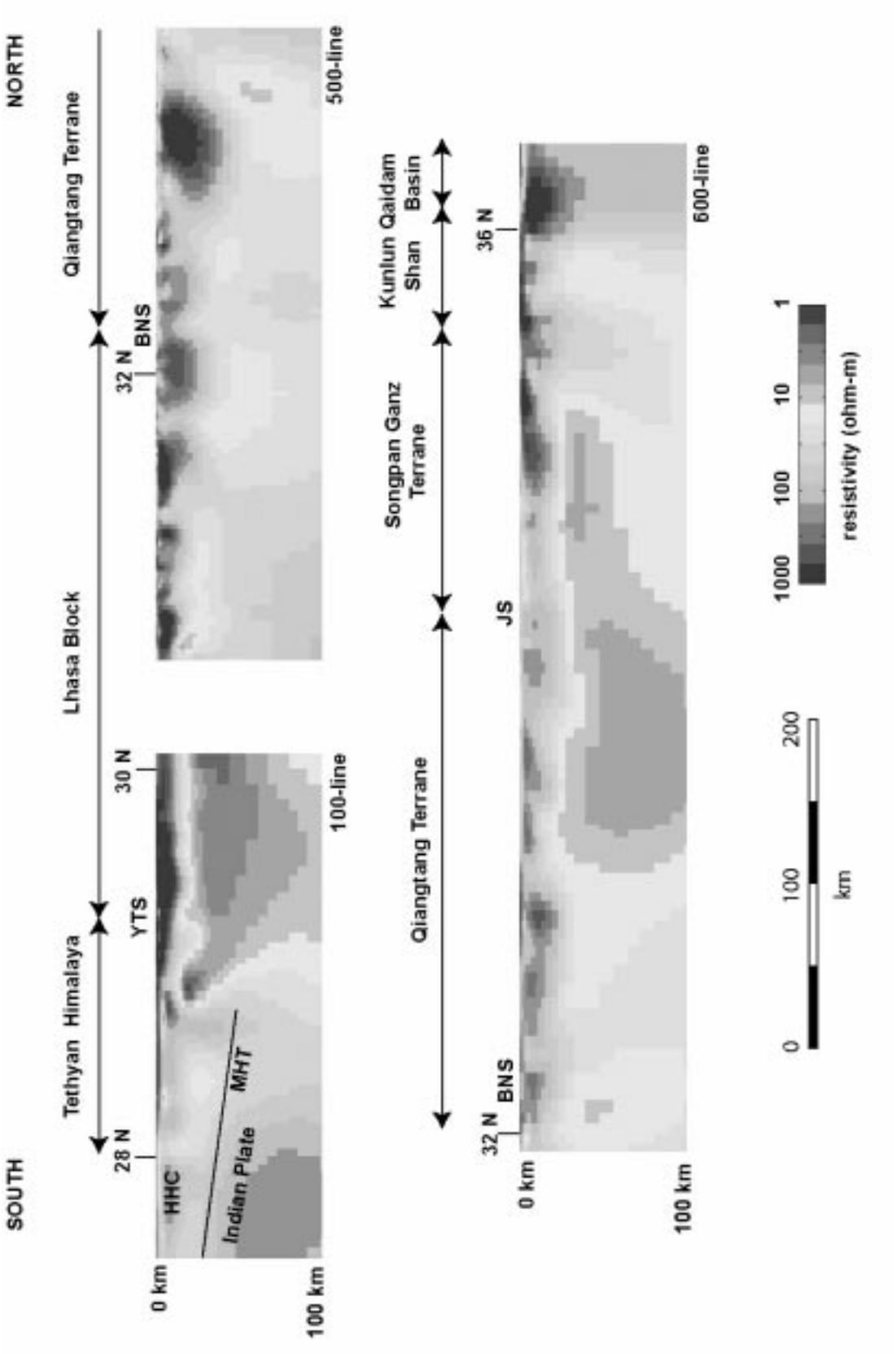

Figure 4. Two dimensional resistivity models derived from the INDEPTH magnetotelluric data. HHC– High Himalayan Crystalline rocks. MHT– Main Himalayan Thrust. BNS – Bangong-Nujiang suture. JS– Jinsha suture. KF– Kunlun Fault. Note also that in parts of Tibet the conductance of the mid crust is so high that the base of the conductive zone cannot be sensed, and the upper conductance bound remains unknown.

produce the observed 10,000 S conductance. Aqueous fluids can be more conductive than melt, and samples from geothermal fields and fluid inclusions show conductivities in excess of 100 S/m (Hyndman & Shearer 1989). Thus a layer of brines could produce the same conductance observed in Tibet with a lower fluid fraction and/or layer thickness than considered above for partial melt. Consider a rock that contains brine with a conductivity of 100 S/m. A layer 1.6 km thick containing 10% brine by volume would be needed to account for the observed 10,000 S conductance. The high conductivity requires that a fluid phase be widespread in the Tibetan crust, but it must be stressed that the MT data alone cannot determine the nature of the fluid. Additional geological and geophysical data are required to distinguish partial melt from brines. It appears that the high conductivity regions in northern and southern Tibet have different characters and this may reflect that are caused by different types of fluid. Seismic data in Tibet also suggest differing crustal structure in the southern and northern parts of the plateau (Owens & Zandt 1997) that have been largely attributed to fluid phases in the crust and upper mantle. In the south the conductor is relatively shallow, confined to the crust and probably due to a combination of aqueous fluids and partial melt (Makovsky & Klemperer 1999). North of the Bangong-Nuijang suture, the mid-crustal conductor is deeper and the top reaches a depth of 40 km. It's base may extend into the mantle, but this is not well constrained by MT data. At these depths, anomalously high conductivity is probably caused by partial melting, since aqueous fluids do not generally form a connected phase under these pressure and temperature conditions. Partial melting of the lower crust and upper mantle is confirmed by the composition of xenoliths collected during the INDEPTH geological mapping program in the Qiangtang Terrane (Hacker *et al.* 2000). Taken together, the seismic, magnetotelluric and geological data suggest that lithospheric delamination is occurring beneath northern Tibet today. This process occurs as cold thickened lithosphere becomes gravitationally unstable and sinks. As localized convection occurs, a zone of hot, upwelling asthenosphere rises to the base of the crust (Molnar *et al.* 1993). The large zone of high conductivity centered at 33.5ºN may represent a zone of upwelling asthenosphere beneath the Qingtang Terrane.

Observations of widespread crustal fluids beneath Tibet are significant because the presence of partial melt or aqueous fluids can mechanically weaken the crust (Cooper & Kohlstedt 1986) and provides a locus for crustal flow. In Southern Tibet, this could effectively decouple the upper and low parts of the crust to permit the continued convergence of India and Asia. In Northern Tibet the conductive lower crust contains sufficient partial melt to weaken it so that lower crustal flow to the east occurs. The termination of the mid-crustal conductor beneath the Kunlun Fault is very significant. The relative motion of the Songpan-Ganze and Qiangtang Terranes may be facilitated by the presence of a weak mid crustal layer to the south of the Kunlun Fault. The zone of relatively high resistivity beneath the Kunlun Shan (600-line, Figure 4) may represent a region where the continental lithosphere has been subducted to the south beneath the Tibetan Plateau.

The tectonic setting of Tibet is very similar to that of Anatolia. In both locations, a north-south continental collision has resulted in a thickened crust that is presently undergoing local east–west motion. Magnetotelluric data collected in western Anatolia have imaged widespread high conductivity in the mid-crust that may imply partial melting has occurred (Gürer 1996; Bayrak *et al.* 2000). It is also significant that the northern limit of this partial melt zone is spatially coincident with the North Anatolian Fault (Gürer 1996), in exactly the same way that the Tibetan partial melt zone terminates at the Kunlun Fault. Continued magnetotelluric exploration in Turkey is needed to further define the electrical structure of the crust and mantle and determine how the rheology is related to ongoing deformation.

Detailed Imaging of Strike-slip Faults

In addition to regional tectonic studies, magnetotellurics can also be used in detailed studies of fault zone structure. Recent studies have suggested that fluids may play a significant role in fault mechanics (Byerlee 1993; Sleep & Blandpied 1992). It has been suggested that zones of over-pressured fluids may account for the apparent weakness of major faults such as the San Andreas Fault (Zoback *et al.* 1987). Since fluids can dramatically lower the resistivity of a rock, a resistivity mapping technique such as magnetotellurics can be used to image spatial and temporal variations in the fluid

distribution within seismically active strike-slip faults. Since 1994 continuous magnetotelluric profiling has been used to study the upper crustal structure of the San Andreas Fault in California. The seismic behavior of the San Andreas Fault is summarized by Wallace (1990) and is quite different to that of the North Anatolian Fault. The northern and southern segments of the San Andreas Fault have been locked since major earthquakes in 1906 and 1857 respectively, while the central section is active creeping and has abundant seismicity up to M= ~ 6. The magnetotelluric technique that was used in California to image fault zone structure differs from that used in Tibet. A high station density was employed to give spatial redundancy in the data. By imaging the near surface structure in great detail, deeper structure can be more reliably defined. Typically a measurement is made every 100 m on a profile that crosses the surface trace of the fault. Over three field seasons, measurements have been on fault segments exhibiting a wide range of seismic behavior. This has included the Carrizo segment that has been locked since 1857, the creeping Central segment near Hollister, and the Parkfield segment. The San Andreas Fault at Parkfield exhibits an intermediate type of behavior with aseismic creep, repeating micro-earthquakes and the characteristic M= 6 events that reoccur approximately every 22 years (Bakun & Lindh 1985). Figure 5 shows the geoelectric structure of the San Andreas Fault at Parkfield, where three high-resolution MT profiles were acquired across the San Andreas Fault (Unsworth *et al.* 1997, 2000). Note the following features of the electrical resistivity model:

(a) Major contrast in electrical resistivity across the fault, with granite to the west exhibiting a much higher resistivity than the Franciscan mélange to the east.

(b) A zone of low resistivity in the fault zone that is probably due to saline ground water in the fractures of the damaged zone and fault core. The resistivities values beneath the trace of the San Andreas Fault imply porosities of 5–30%.

The correlation of the resistivity structure with the distribution of microearthquake hypocenters is striking, suggesting that the earthquakes begin at the base of the conductive (highly fractured) wedge of breccia. Below this depth the fault zone rocks become strong enough to allow sufficient stress to accumulate for small earthquakes to occur. The resistivity variations east of the fault also suggest that on the Parkfield segment, there is

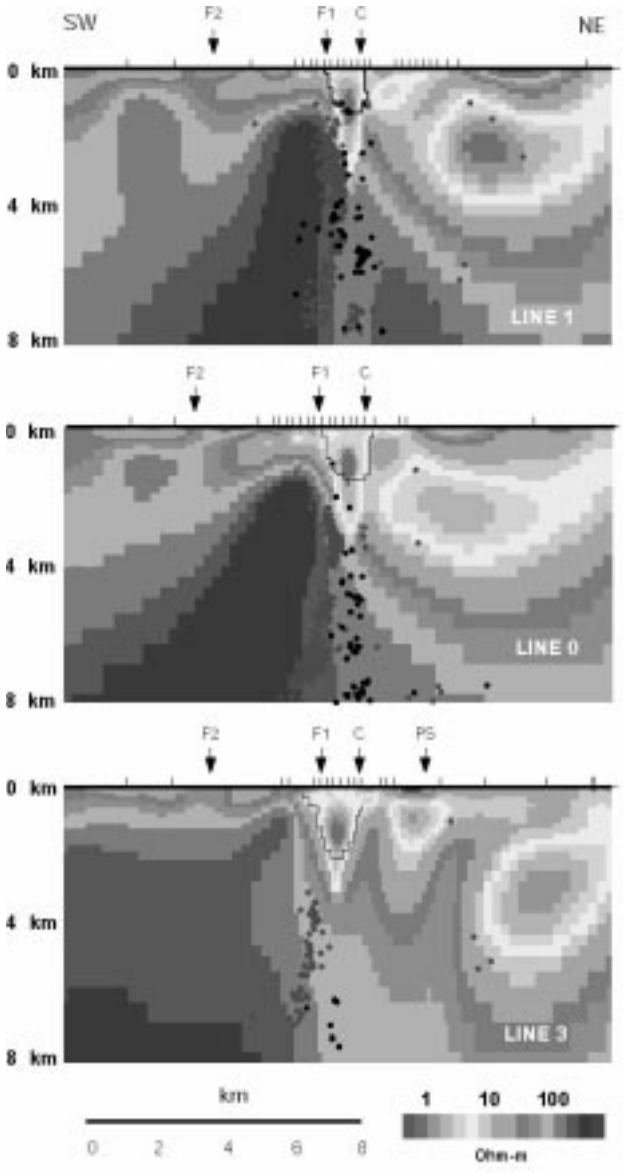

Figure 5. Electrical resistivity models for the three Middle Mountain profiles described by Unsworth *et al.* (2000). Earthquake hypocenters within 2 km of each profile are also shown. Red events are from the Parkfield High Resolution Network (Nadeau & McEvilly 1997) and the black events were relocated by Waldhauser & Ellsworth (1999) from the Northern California Seismic Network. Locations at which MT data were collected are indicated by the black vertical ticks. All conductivity models are shown with no vertical exaggeration. C– surface trace of the San Andreas Fault defined by creep, PS– Parkfield Syncline.

a connection of aquifers in the Franciscan formation (east of the SAF) with the fault zone. The along-strike variation in this fluid supply may be related to the associated changes in seismic behavior. Parkfield is the location for

a 3 km scientific drilling project that will directly sample the properties of the fault zone at depth (Hickman *et al.* 1994). The proposed drill site is on Line 1, approximately 2 km to the west of the surface trace and will allow the San Andreas Fault Observatory at Depth (SAFOD) to be installed. The MT data described in this paper have been used to determine the best location for the hole. Well log information will provide direct confirmation of the resistivity model shown in Figure 5.

In contrast to Parkfield, the San Andreas Fault at Carrizo Plain has a limited zone of high conductivity in the fault zone (Unsworth *et al.* 1999). At this location (approximately 70 km southeast of Parkfield) the San Andreas Fault has been locked since the Fort Tejon earthquake in 1857. Granitic basement was imaged on each of the San Andreas Fault with high electrical resistivities. The fault may be locked at this location by a combination of the low fluid budget (implied by the absence of a major conductivity anomaly in the fault zone) or the presence of mechanically strong crystalline rock on each side of the fault. Alternatively, the granitic basement could act as a fluid flow barrier to keep the fault zone dry, by preventing fluids from the Franciscan formation reaching the San Andreas Fault. To the northwest of Parkfield, the Central segment of the San Andreas Fault is actively creeping. Magnetotelluric data were collected on this segment in 1999 near Hollister and in Bear Valley. Preliminary inversions of these data and show a more extensive fault zone conductor than at Parkfield.

In summary, there is a clear correlation between the electrical resistivity structure and seismic behavior along the San Andreas Fault in central California. It is possible that the high electrical conductivities at Parkfield and Hollister are due to the presence of fault zone fluids that are actually causing the fault to creep. Alternatively, other factors could be controlling which fault segments are locked and which are creeping. In this scenario, the higher electrical conductivities on the creeping segments are due to an extensive network of fluid filled fractures that maintains electrical connection as a result of the continuous deformation. In contrast, the locked Carrizo segment is electrically resistive because cracks that are formed during earthquakes become sealed during the inter-seismic period, and thus the electrical resistivity increases. The existence of this style of variation in a temporal cycle has been suggested by the structural analysis from fault zone rocks on the North Anatolian Fault in Turkey (Janssen *et al.* 1997). A detailed spatial study of fluid distribution in the crust adjacent to the North Anatolian Fault could further elucidate the importance of these processes.

Conclusions

These two studies have shown the ability of modern magnetotelluric exploration to image crustal structure in regions of active tectonic processes. In particular MT has been useful in mapping the fluid distributions in active fault zones and beneath zones of active continental tectonics. The tectonics of California and Tibet share many features in common with western Turkey. The continued application of magnetotellurics to both regional tectonic studies and the detailed investigation of major strike-slip faults in Turkey will bring new insights into the mechanisms of continental dynamics, particularly the role of crustal fluids in the earthquake process and the importance of partial melting in permitting lower crustal flow.

Acknowledgements

The MT fieldwork in Tibet was supported by the U.S. National Science Foundation (Continental Dynamics), the Ministry of Land and Resources of the People's Republic of China, the China University of Geosciences (Beijing) and the Geological Survey of Canada. The fault zone studies in California were supported by the National Science Foundation (Geophysics), the United States Department of Energy and the United States Geological Survey (Earthquake Hazard Reduction Program). Assistance in both MT fieldwork and data analysis from many individuals is gratefully acknowledged.

References

BAKUN, W.H. & LINDH, A.G. 1985. The Parkfield, California, earthquake prediction experiment. *Science* **229**, 619–624.

BAYRAK, M., İLKIŞIK, O.M., KAYA, C. & BAŞOKUR, A.T. 2000. Magnetotelluric data in Western Turkey, dimensionality using Mohr circles. *Journal of Geophysical Research* **105**, 23391–23401.

BROWN, L.D., ZHAO, W., NELSON, K.D., HAUCK, M., ALSDORF, D., ROSS, A., COGAN, M., CLARK, M., X. LIU, X. & CHE, J. 1996. Bright spots, structure and magmatism in Southern Tibet from INDEPTH seismic reflection profiling, *Science* **274**, 1688–1690.

BYERLEE, J. 1993. Model for episodic flow of high-pressure water in fault zones before earthquakes. *Geology* **21**, 303–306.

CAGNIARD, L. 1953. Basic theory of the Magnetotelluric Method of Geophysical Prospecting. *Geophysics* **18**, 605–635.

CHEN, L., BOOKER, J.R., JONES, A.G., WU, N., UNSWORTH, M.J., WENBO, W. & TAN, H. 1996. Electrically Conductive Crust in Southern Tibet from INDEPTH magnetotelluric surveying. *Science* **274**, 1694–1696.

COOPER, R.F. & KOHLSTEDT, D.L. 1986. Rheology and Structure of Olivine-basalt partial melts. *Journal of Geophysical Research* **89**, 9315–9323.

EGBERT, G.D. 1997. Robust multiple station magnetotelluric data processing. *Journal of Geophysical Research* **130**, 475–496.

FRANCHETEAU. J., JAUPART, C., JIE, S., WENHUA, K., DELU, L., JAICHI, B., HUNPIN, W. & HSIAYEU, D. 1984. High heat flow in Southern Tibet. *Nature* **307**, 32–36.

GÜRER, A. 1996. Deep conductivity structure of the North Anatolian Fault Zone and the İstanbul and Sakarya Zones along the Gölpazarı-Akçaova profile, Northwest Anatolia. *International Geology Review* **38**, 727–736.

HACKER, B.R., GNOS, E., RATSCHBACHER, L., GROVE, M., MCWILLIAMS, M., SOBOLEV, S., WAN, J. & WU, Z. 2000. Hot and Dry Deep Crustal Xenoliths from Tibet. *Science* **287**, 2463–2466.

HICKMAN, S., ZOBACK, M.D, YOUNKER, L. & ELLSWORTH, W. 1994. Deep scientific drilling in the San Andreas Fault zone. *EOS Transactions AGU* **5**, 137–139.

HYNDMAN, R.D. & SHEARER, P.M. 1989. Water in the lower continental crust: modeling magnetotelluric and seismic reflection results. *Journal of Geophysical Research* **98**, 343–365.

JANSSEN, C., MICHEL, G.W., BAU, M., LUDERS, V. & MUHLE, K. 1997. The North Anatolian Fault Zone and the role of fluids in seismogenic deformation. *Journal of Geology* **105**, 387–403.

JONES, A.G. 1992. Electrical conductivity of the continental lower crust. *In*: FOUNTAIN, D. ARCHULUS, R.J. & KAY, R. (eds), *The Continental Lower Crust*, 81–143.

KIND, R., NI, J., ZHAO, W., WU, J., YUAN, X., ZHAO, L., SANDOVAL, E., REESE, C., NABELEK, J., HEARN, T. 1996. Evidence from Earthquake data for a partially molten crustal layer in Southern Tibet. *Science* **274**, 1692–1694.

MAKOVSKY, Y. & KLEMPERER, S.L. 1999. Measuring the seismic properties of Tibetan Bright spots: Evidence for free aqueous fluids in the Tibetan Middle crust. *Journal of Geophysical Research* **104**, 10795–10825.

MCNEICE, G.W. & JONES, A.J. 2001. Multisite, multifrequency tensor decomposition of magnetotelluric data. *Geophysics* **66**, 158–173.

MOLNAR, P., ENGLAND, P. & MARTINOD, J. 1993. Mantle dynamics, uplift of the Tibetan Plateau, and the Indian Monsoon. *Reviews of Geophysics* **31**, 357–396.

NADEAU, R. & MCEVILLY, T.V. 1997. Seismological studies at Parkfield V: Microearthquake sequences as Fault-zone drilling targets. *Bulletin of Seismological Society of America* **87**, 1463–1472.

NELSON, K.D., ZHAO, W., BROWN, L.D., KUO, J., CHE, J., LIU, X., KLEMPERER, S.L., MAKOVSKY, Y., MEISSNER, R., MECHIE, J., KIND, R., WENZEL, F., NI, J., NABLEK, J., LESHOU, C., TAN, H., WEI, W., JONES, A.G., BOOKER, J.R., UNSWORTH, M., KIDD, W.S.F., HAUCK, M., ALSDORF, D., ROSS, A., COGAN, M., WU, C. SANDVOL, E., EDWARDS, M. 1996. Partially molten Middle Crust Beneath Southern Tibet: Synthesis of Project INDEPTH results. *Science* **274**, 1684–1686.

OLHOEFT, G.R. 1986. Electrical Properties of Granite with implications for the lower crust. *Journal of Geophysical Research* **86**, 931–936.

OWENS, T.J. & ZANDT, G. 1997. Implications of crustal property variations for models of Tibetan plateau evolution. *Nature* **387**, 37–43.

PARTSCH, G.M., SCHILLING, F.R. & ARNDT, J. 2000. The influence of partial melting on the electrical behavior of crustal rocks: laboratory examinations, model calculations and geological interpretations. *Tectonophysics* **317**, 189–203.

ROBERTS, J.J. & TYBURCZY, J. 1999. Partial melt electrical conductivity: influence of melt composition. *Journal of Geophysical Research* **104**, 7055–7065.

RODI, W. & MACKIE, R.L. 2001. Nonlinear conjugate gradients algorithm for 2-D magnetotelluric inversion. *Geophysics* **66**, 174–187.

SLEEP, N.H. & M.L. BLANDPIED, M.L. 1992. Creep, compaction and the weak rheology of major faults. *Nature* **359**, 687–690.

VAN NGOC, P., BOYER, D., THERME, P., CHENG YUAN, X., LI, L. & YUAN JIN, G. 1986. Partial melting zones in the crust in Southern Tibet from magnetotelluric results. *Nature* **319**, 310–314.

UNSWORTH, M. J., MALIN, P.E., EGBERT G.D. & BOOKER, J.R. 1997. Internal Structure of the San Andreas Fault Zone at Parkfield, California. *Geology* **25**, 359–362.

UNSWORTH, M.J. 1999. Magnetotellurics. *In*: *McGraw-Hill 2000 Yearbook of Science and Technology*, McGraw-Hill, New York, 240–242.

UNSWORTH, M.J., EGBERT G.D. & BOOKER, J.R. 1999. High resolution electromagnetic imaging of the San Andreas Fault in Central California. *Journal of Geophysical Research* **104**, 1131–1150.

UNSWORTH, M.J., EISEL, M., EGBERT, G.D., SIRIPUNARVAPORN, W. & BEDROSIAN, P.A. 2000. Along-strike variations in the structure of the San Andreas Fault at Parkfield, California. *Geophysical Research Letters* **27**, 3021–3024.

VOZOFF, K. 1991. The Magnetotelluric Method. *In*: NABIGHIAN, M.N. (ed), *Electromagnetic Methods in Applied Geophysics*. Society of Exploration Geophysicists Publications, Tulsa, Volume 2, Chapter **8**, 641–711.

WALDHAUSER, F. & ELLSWORTH, W.L. 1999. A double difference earthquake location algorithm: Method and Application to the San Andreas and Hayward Faults, California. *EOS Transactions AGU* **46**, F705.

WALLACE, R. 1990. *The San Andreas Fault System*. US Geological Survey Professional Paper **1515**.

ZOBACK, M.D., ZOBACK, M.L., MOUNT, V.S., SUPPE, J., EATON, J.P., HEALY, J.H, OPPENHEIMER, D., REASENBERG, P., JONES, J., RALEIGH, C.B., WONG, I.G., SCOTTI, O. & WENTWORTH, C. 1987. New evidence on the state of stress of the San Andreas Fault system. *Science* **238**, 1105–1111.

Received 18 February 2002; revised typescript accepted 08 August 2002